Role of Room Temperature Sputtered High Conductive and High Transparent Indium Zinc Oxide Film Contacts on the Performance of Orange, Green, and Blue Organic Light Emitting Diodes

Gonçalo Gonçalves,* Valentina Grasso, Pedro Barquinha, Luís Pereira, Elangovan Elamurugu, Mauro Brignone, Rodrigo Martins, Vito Lambertini, Elvira Fortunato

The core of this paper concerns the use of an amorphous transparent conductive oxide (a-TCO), whose performance is on par with the classical indium tin oxide (ITO) films as a transparent contact in organic light emitting diodes (OLEDs). The main advantage of indium zinc oxide (IZO) films relies on their amorphous structure and high mobility that turns them likely to be used with high conductivity and high transmittance even at the infrared region. The mobility of IZO films ($47.8\,cm^2 \cdot V^{-1} \cdot s^{-1}$) surpasses the one exhibited by ITO films ($26.4\,cm^2 \cdot V^{-1} \cdot s^{-1}$), which along with its smoother surface and better current distribution plays an important role on OLEDs performance. Besides their similar turn-on voltage, the devices using IZO anodes exhibit higher power efficiency than the ITO ones, which is 66, 18, and 62% for orange, green, and blue OLEDs, respectively. These results suggest that IZO can potentially be applied as an anode in full color displays based on OLEDs.

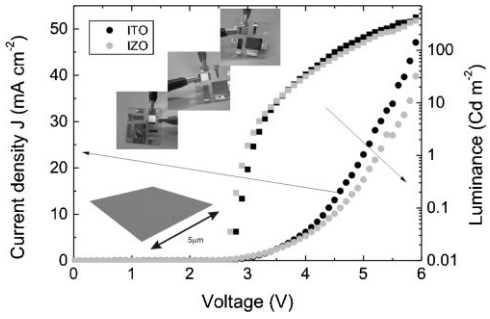

Introduction

Transparent conducting oxides (TCOs) are the key components in a wide range of optoelectronic devices such as solar cells, smart windows, and organic light emitting devices (OLEDs).[1,2] Among the available TCOs, indium tin oxide (ITO) has been widely used owing to its low resistivity, high transparency in the visible region (>80%), and high work function (>4.6 eV).[2–4] However, the increasing interest on ITO alternatives has resulted in a wide range of options including zinc-doped indium oxide (IZO)[4], gallium-doped zinc oxide (GZO),[5,6] and

G. Gonçalves, P. Barquinha, L. Pereira, E. Elamurugu, R. Martins, E. Fortunato
CENIMAT/I3N, Faculdade de Ciências e Tecnologia, Departamento de Ciência dos Materiais, FCT, Universidade Nova de Lisboa and CEMOP-UNINOVA, 2829-516 Caparica, Portugal
E-mail: gpg@fct.unl.pt
V. Grasso, M. Brignone, V. Lambertini
Group Materials Labs, Centro Ricerche Fiat, New Materials Scouting and Nanomaterials, Strada Torino 50, 10043 Orbassano (TO), Italy

DOI: 10.1002/ppap.201000149

aluminum-doped zinc oxide (AZO).[7,8] Among them, IZO is an excellent candidate since it can be deposited at room temperature (RT) using an industry friendly technique such as magnetron sputtering. Furthermore, it exhibits superior properties such as low resistivity ($\approx 10^{-4}\,\Omega \cdot cm^{-1}$), tunable work function (4.7–5.1 eV), high visible transmittance (>80%), smoother surface, and high etching rate.[9] Additionally, it has low compressive stress, which is essential to be used as an electrode in the increasingly developing field of flexible electronics.[10,11]

One of the main applications envisaged for IZO films is their usage as anodes in OLEDs, either polymer light emitting diodes (PLEDs) or small molecule organic light emitting devices (SMOLEDs) for flat panel displays.[12–15] OLEDs are emerging as the next generation front-planes due to their low power consumption, cost effectiveness, high viewing angle, small thickness, and fast response times.[16,17] In this context, full color OLEDs comprising red (R), green (G), and blue (B) pixels need to be fabricated.[16,18,19] Typically there are different approaches to fabricate full color OLED displays: use of lateral emitter, such as side-by-side patterning of discrete R, G, and B sub-pixels, RGB tunable pixels, filtering of white OLEDs, down-conversion of blue emitting OLEDs or filtering of broad-band-emitting OLEDs.[16] It is therefore clear that the TCOs must present a high visible transmittance combined with low resistivity in order to be used in displays. In the present work, we evaluate the structure, morphology, and electro-optical properties of IZO films deposited by RF magnetron sputtering at RT by direct comparison with commercial ITO films. We also demonstrate that IZO is a potential substitute of ITO anode in OLEDs. Thus, three different emissive layers (EMLs) comprising orange, green, and blue were used to cover a wide range of the visible spectrum. The obtained results substantiate that despite the comparable turn-on voltages, devices with IZO are more efficient than those with ITO for all of the EMLs.

Experimental Part

IZO and ITO Substrate Preparation and Characterization

IZO films were deposited onto corning 1 737 glass substrates in a home-made RF magnetron sputtering at RT using a 3″ ceramic oxide target (In_2O_3/ZnO, 2:1 mol) from SCM, Inc., with a purity of 99.99%. The oxygen partial pressure and the deposition pressure ($Ar + O_2$) were kept constant at 1.5×10^{-3} Pa and 2×10^{-1} Pa, respectively. In order to assure high reproducibility, the base pressure was maintained constant at 3×10^{-4} Pa. The target–substrate distance and RF power were kept constant at 15 cm and 75 W, respectively. The commercial ITO substrates from Unaxis were used as reference for the comparative study.

The thickness of IZO (220 nm) and ITO (130 nm) was measured by profilometry using an Ambios XP-200 profiler. The films' structure was confirmed by X-ray diffraction using a Panalytical X'Pert PRO in Bragg-Brentano ($\theta/2\theta$ coupled) geometry with Cu Kα line radiation ($\lambda = 1.540598$ Å). The surface morphology was investigated using scanning electron microscopy (FE-SEM, Zeiss Auriga Crossbeam microscope). Conductive atomic force microscopy (C-AFM), using a MFP-3D AFM from Asylum was utilized for collecting simultaneous topography and current imaging for the purpose of evaluating the morphology and the current distribution on the films' surface. The C-AFM operates in contact mode by using a conductive AFM tip (Si probe for contact mode with Pt Coating, OMCL-240TM, from Olympus). The Z feedback loop uses the DC cantilever deflection signal to maintain a constant force between the tip and the sample, to generate a topography image. Simultaneously, a DC bias is applied to the tip to generate a current image. The electrical properties were measured using BioRad HL5500 Hall effect system in Van der Pauw geometry at RT, with a 0.5 T constant magnetic field. The transmittance spectra (300–2 100 nm) were obtained from a double beam spectrophotometer (UV 3100PC, Shimadzu). The work function of the films was evaluated by Kelvin Probe method in air using a KP Technology system. The experiment was conducted in 5 points on the surface of each sample (4 points in the corner of a square and the 5th point at the center) and each measurement was repeated 10 times.

Devices Fabrication and Characterization

IZO and commercial ITO deposited on glass with a sheet resistance of 22 and 12 Ω/sq, respectively, were cleaned by sonication in a Micro90 solution for 10 min. Subsequently, anodes were sonicated sequentially in acetone and 2-propanol, and finally dried by blowing nitrogen. In order to increase the device efficiency, 50 nm thick hole injection layer of PEDOT: PSS (Baytron Al4083 from HCStarck) was spin-coated on the different anodes and dried in air at 90 °C. Spin-coated 90 nm thick PPV based polymers with blue, green, and orange emission were used as emitting layers. The cathode was defined by thermally evaporating a 150 nm thick layer of Ca/Al alloy through a shadow mask with four square openings of different sizes. All the substrates had four active emitting areas of 4, 16, 36, and 100 mm^2, from which the 36 mm^2 area was selected for characterization. The electro-optical properties were obtained through *I–V–L* curves and power efficiency ($lm \cdot W^{-1}$) in air. The electrical behavior was investigated using Keithley K2425 source meter. The devices are connected to the source/meter and during the *I–V* characterization the light emitted from the device is collected by a photodiode connected with an integrated sphere.

Results and Discussion

Structural and Morphological Characterization

The XRD patterns obtained for ITO and IZO thin films are depicted in Figure 1. The obtained patterns confirmed the standard cubic ITO structure (ICDD File no.: 98-005-1984), for ITO films. The obtained diffraction peaks were identified as (112), (222), (233), (134), and (044) plans by matching with the standard data. The crystallite size estimated from

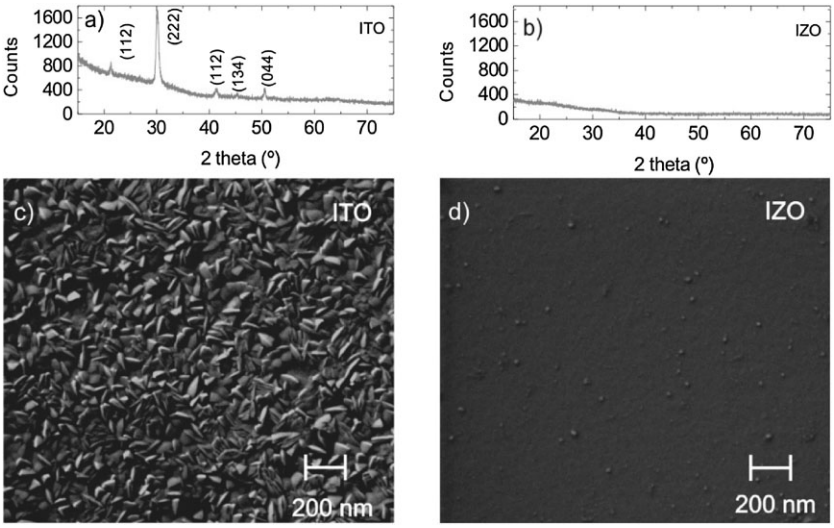

Figure 1. XRD patterns obtained from (a) ITO and (b) IZO thin films; SEM microstructures obtained from (c) ITO and (d) IZO thin films.

the high intensity (222) peak using Debye–Scherrer equation ranges between 18 and 21 nm. The obtained polycrystalline structure presumably arises from the high processing or post-annealing temperatures used in commercial sputtering processes.[20,21] On the other hand, IZO films present only a halo peak, characteristic of amorphous/nano-crystalline structures.[22,23] In fact, during the deposition of IZO films, the substrate was not intentionally heated and the temperature was maintained below 100 °C. Such low temperature usually results in the formation of an amorphous structure. Contrarily to ITO, another advantage of IZO is that its amorphous structure can be preserved even after annealing at temperatures as high as 400–500 °C (depending on composition and deposition conditions), as shown in previous publications.[20,22]

The SEM micrograph of ITO (Figure 1c) is comprised of "rice-like" grains, with lateral top sizes ranging between 60 and 80 nm. These grains are randomly oriented, which corroborates the polycrystalline structure confirmed by XRD analysis. In contrast, the microstructure obtained for IZO films shows a much smoother surface with no remarkable features on the surface which is coherent with the amorphous/nano-crystalline structure suggested by XRD analysis.

Figure 2 shows the surface morphology (3D) and electrical current images (5 μm × 5 μm) of ITO and IZO thin-films obtained by C-AFM. For ITO films the surface is comprised of uniformly sized cubical shaped grains, with lateral top sizes varying between 74 and 95 nm. However, the grains are not packed tightly and that presumably influences the root-mean-square (RMS) roughness, which is 2.7 nm. On the other hand, the surface of IZO films present small grains that are closely packed. The RMS roughness of IZO films (0.7 nm) is about 75% smaller than ITO films. C-AFM images show a different current distribution on IZO compared with ITO. A more homogeneous distribution of the current density was observed on the surface of IZO films as it is desirable in OLEDs, since it increases the brightness homogeneity, especially in large area devices.[24,25] The current image of ITO thin films shows a more heterogeneous distribution with paths of high conductivity surrounded by very low conductivity regions.

Electrical Properties

The electrical properties of IZO and ITO films were measured by Hall Effect. The bulk resistivity (ρ) of $4.29 \times 10^{-4}\,\Omega \cdot cm^{-1}$ obtained for the IZO films is slightly higher than that of commercial ITO films ($1.59 \times 10^{-4}\,\Omega \cdot cm^{-1}$). The obtained Hall sign suggests that both films are predominantly electron transporting. The striking feature is that the mobility of IZO films ($47.8\,cm^2 \cdot V^{-1} \cdot s^{-1}$) is almost double than that of ITO films ($26.4\,cm^2 \cdot V^{-1} \cdot s^{-1}$). ITO films show a carrier concentration of $1.41 \times 10^{21}\,cm^{-3}$, which is about

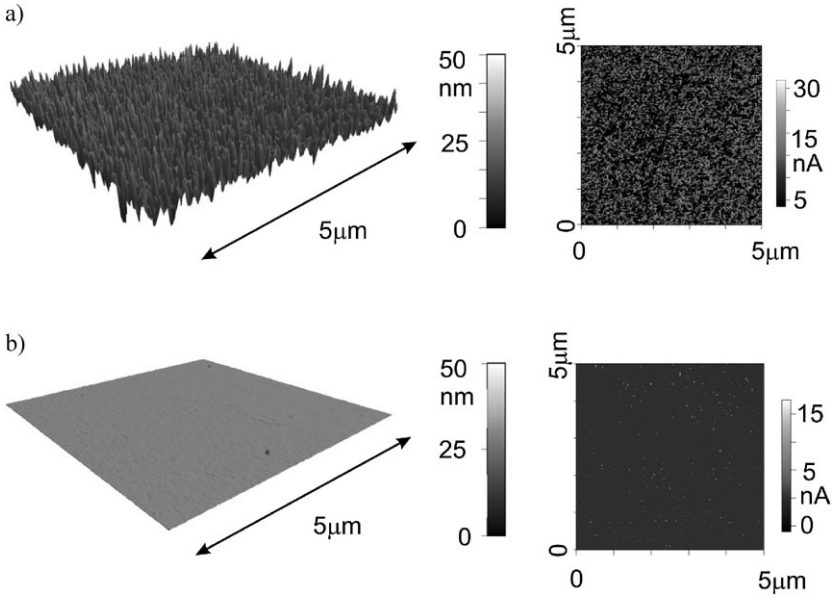

Figure 2. High-resolution topography image and simultaneous current image obtained from (a) ITO at a bias of 10 mV and (b) IZO at bias of 4 V.

DOI: 10.1002/ppap.201000149

one order of magnitude higher than that of IZO films ($3.04 \times 10^{20}\,cm^{-3}$). The obtained values suggest that both films are highly degenerated TCOs.[26] The scattering of charge carriers, which dominates the mobility on these films, can be attributed to diverse factors such as grain boundaries, lattice vibrations, and ionized and neutral impurities.[27] In IZO films with mobilities exceeding $47\,cm^2 \cdot V^{-1} \cdot s^{-1}$, ionized impurities are the primary cause for the scattering of charge carriers.[26,27] The same scattering mechanism is found in highly degenerated ITO films, similar to the ones studied in this work.[28] Besides the different structural properties mentioned before the fact that the carrier concentration in ITO is about one order of magnitude higher than in IZO might explain the higher dispersion of the free carriers and hence lower mobility for ITO.

Optical Properties

The transmittance spectra obtained from IZO and ITO films in wavelengths ranging from 300 to 2 200 nm are shown in Figure 3. The average visible transmittance (400–800 nm) of ITO films (85%) is slightly higher than that of IZO films (82%). In the near infrared (NIR) region (800–2 200 nm) the optical transmission of these films is typically related to the photon interaction with the free electrons.[29,30] In NIR region, IZO films are more transparent than ITO, due to the lower carrier concentration of the former. The optical band gap (E_{op}) was estimated using the Tauc relation: $\alpha^x = (h\upsilon - E_{op})$, where α represents the absorption coefficient, h the Planck's constant, and υ the photon frequency. For highly degenerated conductive oxides the direct allowed transition is normally applied, hence $x = 2$. E_{op} is estimated from the x-axis intercept of the α^2 versus $h\upsilon$ plot (inset of Figure 3), by extrapolating the linear region of the curve until $y = 0$.[30] It is observed that E_{op} of ITO (3.96 eV) is higher than IZO (3.80 eV). Additionally, the rise of α with $h\sigma$ is sharper for ITO, which is consistent with different structural properties: in polycrystalline materials band transitions occur for well-defined energies while in amorphous materials they occur for a broader energy range.

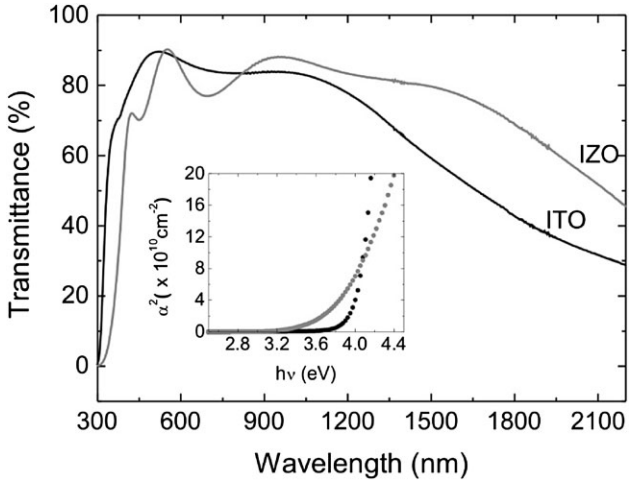

Figure 3. Comparison of transmittance spectra obtained from IZO and ITO films (inset shows the estimation of E_{op}).

Devices Characterization

In this work, we focused on the performance of OLEDs with orange, green, and blue EMLs, using IZO and ITO as testing and reference anodes, respectively. Figure 4 compares

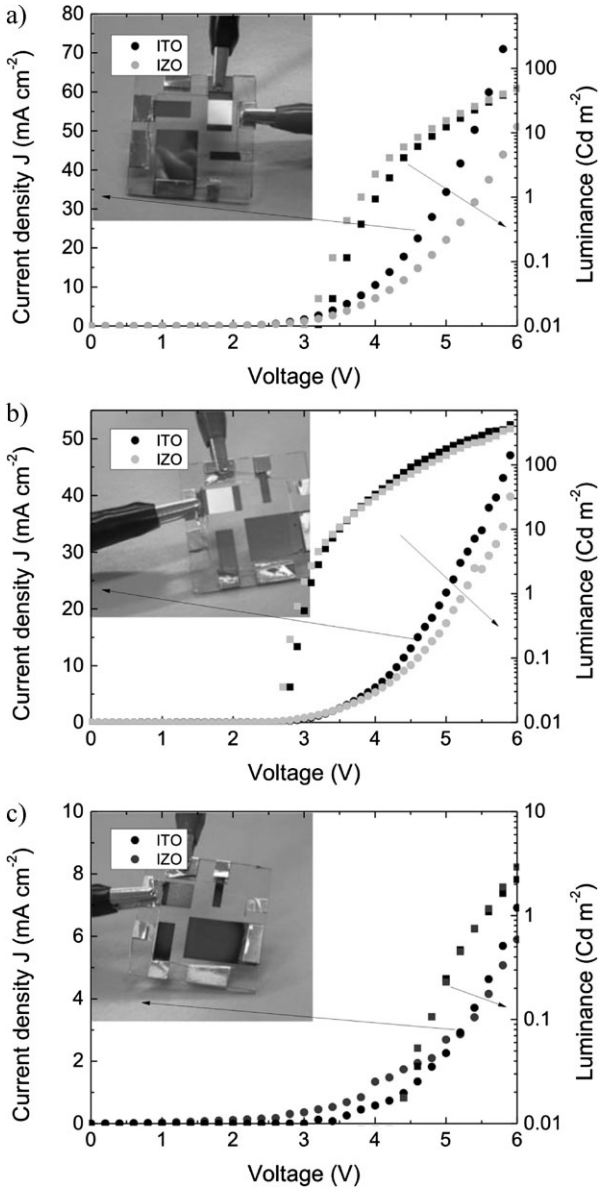

Figure 4. Current–voltage–luminance (I–V–L) of (a) oxide/PEDOT:PSS/orange emitter/ Ca–Al; (b) oxide/PEDOT:PSS/green emitter/ Ca–Al; (c) oxide/PEDOT:PSS/ blue emitter/ Ca–Al; The oxide refers to either IZO or ITO anode.

the *I–V–L* characteristics with the following structures: (Figure 4a) oxide/PEDOT:PSS/orange emitter/Ca–Al; (Figure 4b) oxide/PEDOT:PSS/green emitter/Ca–Al; (Figure 4c) oxide/PEDOT:PSS/blue emitter/Ca–Al. For each structure two devices were made, one with the IZO films deposited in the present study (22 Ω/sq), the other with commercial ITO (12 Ω/sq). The *I–V* and *L–V* curves show a typical diode behavior, with current and power output observed in the forward bias.

It is found that the work function of 5.12 eV obtained from IZO anodes is almost identical to the one of ITO (5.05 eV). This suggests that both anodes should inject nearly the same amount of carriers into the organic layer.[31] The work function of the anode combined with the highest occupied molecular orbital (HOMO) level of the hole transporting layer (HTL), PEDOT/PSS, determines the hole injection barrier in an OLED. The height of this barrier plays an important role in determining the operation voltage of the devices.[31–33] Besides that, the surface chemistry and morphology are known to have a remarkable effect on charge injection in the TCO/organic interface.[32] In particular, the formation of surface dipoles due to interfacial chemical reaction, charge transfer across the interface, and other types of rearrangement of the electronic charge dramatically changes the height of this barrier.[31,34] It has been reported that the formation of surfaces dipoles improves the performance of OLEDs by improving the work function of the anode.[35,36]

The turn-on voltage and luminance of both anodes is in the same order of magnitude for the three EMLs. However, IZO devices exhibit a slightly lower turn-on voltage suggesting a better TCO/organic interface. The device parameters are summarized in Table 1.

Besides the TCO/organic interface, the EML also plays an important role on the devices performance. Actually, the results show that the blue OLEDs present the highest turn-on voltage and the lowest luminance, while the opposite happens in the case of the green OLEDs. This is presumably arising from the mismatch between the energy levels of the different layers, i.e., HOMO level of HTL and HOMO level of EML/and Fermi level of the cathode and lowest unoccupied molecular orbital (LUMO) level of the EML.[37,38] Nevertheless, since the devices were made and tested in atmospheric conditions, the degradation of the organic layers as well as the cathode have a strong influence on the devices performance.[39] Besides that, it is important to stress that the devices using IZO anodes present the highest power efficiency for the three EMLs. Moreover, the superior power efficiency of IZO based devices compared with ITO is attributed to a better charge balance, which in principle should lead to a change in the position of the recombination zone.[13,40]

Table 1. Summary of OLED performance using IZO and ITO anodes with orange, green, and blue emitters.

Emitter	Orange		Green		Blue	
Anode	ITO	IZO	ITO	IZO	ITO	IZO
Turn-on voltage (V)	3.2	3.0	2.8	2.7	4.5	4.2
Power efficiency ($lm \cdot W^{-1}$)	0.3	0.5	4.4	5.2	0.016	0.026

Conclusion

In this paper we have presented the properties of commercial ITO and RT sputtered IZO thin films and their influence on OLEDs performance. ITO films showed a polycrystalline structure along with a rough surface (R_{rms}, 2.7 nm). On the other hand, IZO films exhibited an exceptionally smooth surface (R_{rms}, 0.7 nm) due to its amorphous structure.

The electrical characterization demonstrated that, besides the comparable resistivity ($10^{-4}\,\Omega \cdot cm^{-1}$) of both films, IZO films presented a high mobility ($47.8\,cm^2 \cdot V^{-1} \cdot s^{-1}$) that is almost double than that of ITO ($26.4\,cm^2 \cdot V^{-1} \cdot s^{-1}$). The high mobility of IZO films enhanced the high transmittance toward the NIR region spectra as demonstrated by the optical properties.

The devices produced showed that the different properties exhibited by the films play an important role on the devices performance. Namely, the smooth surface and the high mobility of IZO films resulted in OLEDs with high power efficiency (when compared with ITO) and low turn-on voltages (<4.5 V) for all colors (orange, green, and blue).

We denote that IZO is a promising anode material, which can potentially replace the conventional ITO anode in full color displays based on OLEDs. Furthermore, the possibility of processing IZO anodes at low temperatures will play a vital role in producing flexible displays.

Acknowledgements: The authors Gonçalo Gonçalves and Elangovan Elamurugu acknowledge *Fundação para a Ciência e a Tecnologia (FCT-MCTES)* for offering research grants through the fellowships SRFH/BD/27313/2006 and SFRH/BPD/35055/2007, respectively. This work was partially supported by the *European Commission* under projects INVISIBLE (advanced grant from *ERC* contract no. 228144), *MULTIFLEXIOXIDES* (NMP3-CT-2006-032231) and *EUNIMAfab* (FP7-226460) and by *FCT-MCTES* through the projects PTDC/CTM/73943/2006 and PTDC/EEA-ELC/64975/2006.

Received: October 19, 2010; Revised: January 3, 2011; Accepted: January 13, 2011; DOI: 10.1002/ppap.201000149

Keywords: indium zinc oxide; OLEDs; optoelectronic devices; oxides; sputtering

DOI: 10.1002/ppap.201000149

[1] E. Fortunato, D. Ginley, H. Hosono, D. C. Paine, *Mrs Bull.* **2007**, *32*, 242.
[2] C. G. Granqvist, A Hultåker, *Thin Solid Films* **2002**, *411*, 1.
[3] E. Fortunato, L. Raniero, L. Silva, A. Goncalves, A. Pimentel, P. Barquinha, H. Aguas, L. Pereira, G. Goncalves, I. Ferreira, E. Elangovan, R. Martins, *Solar Energy Mater. Solar Cells* **2008**, *92*, 1605.
[4] E. Fortunato, A. Pimentel, A. Gonçalves, A. Marques, R. Martins, *Thin Solid Films* **2006**, *502*, 104.
[5] E. Fortunato, V. Assuncao, A. Goncalves, A. Marques, H. Aguas, L. Pereira, I. Ferreira, P. Vilarinho, R. Martins, *Thin Solid Films* **2004**, *451*, 443.
[6] J. J. Berry, D. S. Ginley, P. E. Burrows, *Appl. Phys. Lett.* **2008**, *92*, 193304.
[7] K. H. Kim, K. C. Park, D. Y. Ma, *J. Appl. Phys.* **1997**, *81*, 7764.
[8] H. Kim, C. M. Gilmore, J. S. Horwitz, A. Pique, H. Murata, G. P. Kushto, R. Schlaf, Z. H. Kafafi, D. B. Chrisey, *Appl. Phys. Lett.* **2000**, *76*, 259.
[9] K. Ramamoorthy, K. Kumar, R. Chandramohan, K. Sankaranarayanan, *Mater. Sci. Eng. B-Solid State Mater. Adv. Technol.* **2006**, *126*, 1.
[10] E. Fortunato, P. Barquinha, L. Pereira, G. Goncalves, R. Martins, "*Advanced materials for the next generation of thin film transistors*" In: Idmc'07: Proceedings of the International Display Manufacturing Conference, C. H. Chen, Y. S. Tsai, Eds., 2007, Taipei: Society Information Display Taipei Chapter 2007: 371.
[11] M. P. Taylor, D. W. Readey, M. van Hest, C. W. Teplin, J. L. Alleman, M. S. Dabney, L. M. Gedvilas, B. M. Keyes, B. To, J. D. Perkins, D. S. Ginley, *Adv. Funct. Mater.* **2008**, *18*, 3169.
[12] J. H. Bae, J. M. Moon, S. W. Jeong, J. J. Kim, J. W. Kang, D. G. Kim, J. K. Kim, J. W. Park, H. K. Kim, *J. Electrochem. Soc.* **2008**, *155*, J1.
[13] G. Bernardo, G. Goncalves, P. Barquinha, Q. Ferreira, G. Brotas, L. Pereira, A. Charas, J. Morgado, R. Martins, E. Fortunato, *Synth. Met.* **2009**, *159*, 1112.
[14] J. W. Kang, W. I. Jeong, J. J. Kim, H. K. Kim, D. G. Kim, G. H. Lee, *Electrochem. Solid State Lett.* **2007**, *10*, J75.
[15] H. K. Kim, *Surf. Coat. Technol.* **2008**, *203*, 652.
[16] B. Geffroy, P. Le Roy, C. Prat, *Polym. Int.* **2006**, *55*, 572.
[17] Y. Shirota, *J. Mater. Chem.* **2000**, *10*, 1.
[18] M. C. Gather, A. Kohnen, A. Falcou, H. Becker, K. Meerholz, *Adv. Funct. Mater.* **2007**, *17*, 191.
[19] F. Ventsch, M. C. Gather, K. Meerholz, *Org. Electron.* **2010**, *11*, 57.
[20] G. Goncalves, E. Elangovan, P. Barquinha, L. Pereira, R. Martins, E. Fortunato, *Thin Solid Films* **2007**, *515*, 8562.
[21] H. Morikawa, M. Fujita, *Thin Solid Films* **2000**, *359*, 61.
[22] M. P. Taylor, D. W. Readey, M. van Hest, C. W. Teplin, J. L. Alleman, M. S. Dabney, L. M. Gedvilas, B. M. Keyes, B. To, J. D. Perkins, D. S. Ginley, *Adv. Funct. Mater.* **2008**, *18*, 3169.
[23] R. Martins, P. Barquinha, A. Pimentel, L. Pereira, E. Fortunato, *Phys. Status Solidi A-Appl. Mater. Sci.* **2005**, *202*, R95.
[24] C. Garditz, A. Winnacker, F. Schindler, R. Paetzold, *Appl. Phys. Lett.* **2007**, *90*, 103506.
[25] C. Piliego, M. Mazzeo, M. Salerno, R. Cingolani, G. Gigli, A. Moro, *Appl. Phys. Lett.* **2006**, *89*, 103514.
[26] A. J. Leenheer, J. D. Perkins, M. F. A. M. van Hest, J. J. Berry, R. P. O'Hayre, D. S. Ginley, *Phys. Rev. B* **2008**, *77*, 115215.
[27] H. R. Fallah, M. Ghasemi, A. Hassanzadeh, H. Steki, *Mater. Res. Bull.* **2007**, *42*, 487.
[28] H.-C. Lee, *Appl. Surf. Sci.* **2006**, *252*, 3428.
[29] T. Osada, T. Kugler, P. Broms, W. R. Salaneck, *Synth. Met.* **1998**, *96*, 77.
[30] I. Hamberg, C. G. Granqvist, *J. Appl. Phys.* **1986**, *60*, R123.
[31] H. Ishii, K. Sugiyama, E. Ito, K. Seki, *Adv. Mater.* **1999**, *11*, 605.
[32] N. Koch, A. Elschner, J. Schwartz, A. Kahn, *Appl. Phys. Lett.* **2003**, *82*, 2281.
[33] A. Moujoud, S. H. Oh, K. Y. Heo, K. W. Lee, H. J. Kim, *Org. Electron.* **2009**, *10*, 785.
[34] M. Nakano, A. Tsukazaki, R. Y. Gunji, K. Ueno, A. Ohtomo, T. Fukumura, M. Kawasaki, *Appl. Phys. Lett.* **2007**, *91*, 142113.
[35] C. C. Wu, C. I. Wu, J. C. Sturm, A. Kahn, *Appl. Phys. Lett.* **1997**, *70*, 1348.
[36] J. S. Kim, M. Granstrom, R. H. Friend, N. Johansson, W. R. Salaneck, R. Daik, W. J. Feast, F. Cacialli, *J. Appl. Phys.* **1998**, *84*, 6859.
[37] L. Wang, D. W. Matson, E. Polikarpov, J. S. Swensen, C. C. Bonham, L. Cosimbescu, J. J. Berry, D. S. Ginley, D. J. Gaspar, A. B. Padmaperuma, *J. Appl. Phys.* **2010**, *107*, 043103.
[38] H. Aziz, Z. D. Popovic, N.-X. Hu, A.-M. Hor, G. Xu, *Science* **1999**, *283*, 1900.
[39] A. P. Ghosh, L. J. Gerenser, C. M. Jarman, J. E. Fornalik, *Appl. Phys. Lett.* **2005**, *86*, 3.
[40] J. F. Li, S. H. Su, K. S. Hwang, M. Yokoyama, *J. Phys. D, Appl. Phys.* **2007**, *40*, 2435.